International Journal of Scientific Engineering and Science
Volume 5, Issue 2, pp. 62-72, 2021. ISSN (Online): 2456-7361

Development of Mathematical Model for Carbon Dioxide Produced using Oxygen Diffusion for Bioremediation of Petroleum Contaminated Soils

Uchendu Umeda, Yamainian T. Puyate, Emmanuel O. Ehirim, Lloyd G. Amagbo
Department of Chemical/Petrochemical Engineering Rivers State University, Port Harcourt, Nigeria
Email address: umexil @ yahoo.com

Abstract— *In this research, a mathematical model was developed to study the generation of carbon dioxide using oxygen diffusion as a method in bioremediation of petroleum contaminated soils at 100cm depth. The predictability of carbon dioxide concentration by the model was tested in three types of soils: sandy, sandy loam and clay soils, which were polluted with Bonny Light Crude oil and transferred into reactors with dimension 20cm x 100cm. The mathematical model in two dimensional flows (x and z) was developed from basic conservative principle and it was solved numerically to obtain the final solution. MATLAB 8.5 version (R2015a) was used to simulate the model, predicting carbon dioxide concentration along longitudinal and transverse direction of carbon dioxide generation during the bioremediation of petroleum contaminated soils at 100cm depth. The results from the model were compared with experimental results and both showed good fit at all data point. Therefore, the developed model can be used for predicting the concentration of carbon dioxide produced as a byproduct in bioremediation of petroleum contaminated soils.*

Keywords— *Bioremediation, Carbon dioxide, Dimensional flow and Mathematical Model*.

I. INTRODUCTION

Bioremediation is a process that offers the possibilities to destroy or render various contaminants harmless, using natural biological activities (Vidali, 2001). Bioremediation involves three principal approaches namely, natural attenuation, bio-stimulation and bio-augmentation (Chikere *et al*., 2009a). For effective bioremediation to take place in soil, there must be sufficient nutrient and oxygen concentration in soil to enhance the activities of microorganism (Umeda *et al*., 2017). Nutrients are easily assimilated by soil microorganisms in soil pollution with crude oil, thus reducing the nutrient reserves (Rahman *et al*., 2002). Petroleum biodegradation is highly dependent on environmental conditions and on the chemical structure of the pollutant compounds (Swannell *et al*., 1996; Aldrett *et al*., 1997). The rates of degradation and the quality of hydrocarbon eliminated also depend on the type and amount of hydrocarbon present at the contaminant site (Del Arco & de Franca, 2001). Components that are low in molecular weight such as the aliphatic hydrocarbons tend to be degraded first, leaving behind the much larger molecules (aromatic hydrocarbon) which take much longer to break down. The lighter carbon components of the crude oil are also less viscous and can easily degrade and become volatile when acted upon by weather and environmental elements. This trend indicates the presence of biodegradation by microbial bacteria which cannot break down the larger oil compounds left after the initial phases of degradation (Ezra *et al*., 2000). Hydrocarbons from crude oil are substrates for microorganisms, hence, when an accidental oil spill occurs, the number of hydrocarbon degrading microorganisms in the ecosystem increases. The speed and efficiency of bioremediation of soil contaminated with petroleum and petroleum products depend on the number of hydrocarbon-degrading microorganisms in the soil. The most important factors for population growth are temperature, oxygen, pH, content of nitrogen and phosphorus, hydrocarbon class and their effective concentration. Also, the degree and rate of biodegradation are influenced by the type of soil in which the process occurs (Van hmm *et al*., 2003).

Because oxygen played important role in biodegradation of hydrocarbon in soil, it is imperative therefore, to study the diffusion of oxygen in soil polluted by hydrocarbon content. Previous studies have demonstrated the usefulness of mathematical model in the study of gaseous diffusion in soil (Jose *et al*., 2015). Though, some of these models deviated from reality owning to soil heterogeneous properties such as texture and structure of the porous media (Obando, 2003). However, approximate prediction of gas diffusion into soil can be made through the application of the Fick's laws, by accurately accounting for the factors relating to the characteristics of the pore matrix like the diffusion coefficient (Moldrup *et al.* 2013). Hence, when the coefficient of the diffusing gas is precisely predicted, oxygen diffusion can as well be accurately predicted, although, the coefficient may be different for different soil (Abdulsalam, 2012). Thus, in this study, the diffusion of oxygen in sandy, sandy loam and clay soils polluted with hydrocarbon was studied to determine the concentration of carbon dioxide produced during bioremediation of petroleum contaminated soils using a mathematical model.

II. DEVELOPMENT OF MATHEMATICAL MODEL

Mathematical model for oxygen diffusion through petroleum contaminated soils in two dimensional flows (x and z) was developed from basic conservative principle as shown below.

http://ijses.com/
All rights reserved

International Journal of Scientific Engineering and Science
Volume 5, Issue 2, pp. 62-72, 2021. ISSN (Online): 2456-7361

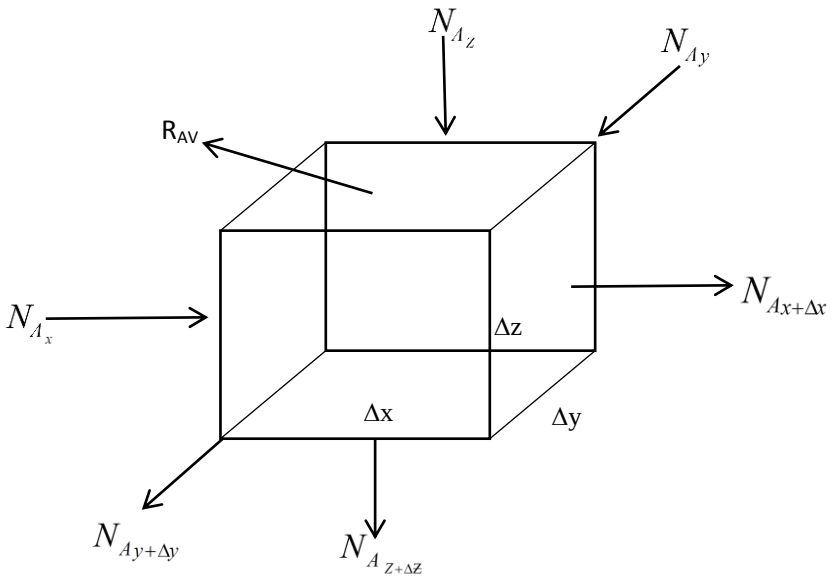

Figure 1a: Hypothetical control volume showing the diffusion of oxygen in soil

Considering the conservation of Species '**A'** including production of **A** by chemical reaction within the volume, the general relation for mass balance of component **A** for the control volume is stated as:

$$\begin{bmatrix}\text{Net rate of mass}\\ \text{efflux of A from}\\ \text{control volume}\end{bmatrix}+\begin{bmatrix}\text{Net rate of}\\ \text{Acceleration of A}\\ \text{within control volume}\end{bmatrix}-\begin{bmatrix}\text{Rate of chemical}\\ \text{production of A within}\\ \text{the control volume}\end{bmatrix}=0 \qquad (1)$$

Defining individual terms in equation (1) and deriving from basic conservative principle, we obtain the following. The net rate of mass efflux from the control volume could be evaluated by considering the mass transferred across control surfaces. Hence, the mass of component **A** transferred across the area can be expressed as:

ΔyΔz at *x* will be $\rho_A V_{Ax}\Delta y\Delta z / x$ (2)

That is $n_{Ax}\Delta y\Delta z / x$.

The net rate of mass efflux of component **A** in the *x*-direction will be:

$$n_{Ax}\Delta y\Delta z /_{x+\Delta x} - n_{Ax}\Delta y\Delta z /_{x} \qquad (3)$$

Similarly in the *y* - direction: $n_{Ay}\Delta y\Delta z / y+\Delta y - n_{Ay}\Delta y\Delta z / y$ (4)

In the *z* - direction: $n_{Az}\Delta x\Delta y / z+\Delta z - n_{Az}\Delta x\Delta y / z$ (5)

Rate of accumulation of volume **A** with control = $\frac{\partial \rho_A}{\partial t}\Delta x\Delta y\Delta z$ (6)

Rate of reaction by chemical reaction = $r_A\Delta x\Delta y\Delta z$ (7)

Substituting equations (2) through (7) into equation (1), we obtained:

$$n_{Ax}\Delta y\Delta z / x+\Delta x - n_{Ax}\Delta y\Delta z / x + n_{Ay}\Delta x\Delta z / y+\Delta y - n_{Ay}\Delta x\Delta z / y + n_{Az}\Delta x\Delta y / z+\Delta z - n_{Az}\Delta x\Delta y / z +$$

$$\frac{\partial \rho_A}{\partial t}\Delta x\Delta y\Delta z - \gamma_A\Delta x\Delta y\Delta z = 0 \qquad (8)$$

Dividing through by the volume $\Delta x\Delta y\Delta z$, and cancelling terms, we have

$$\frac{\eta_{AX}/x+\Delta x - n_{Ax}/x}{\Delta x}+\frac{n_{Ay}/y+\Delta y - n_{Ay}/y}{\Delta y}+\frac{n_{AZ}/z+\Delta z - n_{Az}/z}{\Delta z}+\frac{\partial \rho_A}{\partial t}-\rho_A=0 \qquad (9)$$

Taking limit as $\Delta x, \Delta y$ and Δz approaches zero, this yields:

$$\frac{\partial \eta_{Ax}}{\partial x}+\frac{\partial \eta_{Ay}}{\partial y}+\frac{\partial \eta_{Az}}{\partial z}+\frac{\partial \rho_A}{\partial t}-r_A=0 \qquad (10)$$

http://ijses.com/
All rights reserved

Equation (10) is the continuity equation for component **A**, and η_{Ax}, η_{Ay} and η_{Az} are the rectangular components of the mass flux vector. Therefore, equation (10) may be written

$$\nabla n_A + \frac{\partial \rho_A}{\partial t} - r_A = 0 \quad (11)$$

Similarly, the continuity equation for component **B** can be expressed in the same manner as:

$$\frac{\partial n_{Bx}}{\partial x} + \frac{\partial n_{By}}{\partial y} + \frac{\partial n_{Bz}}{\partial z} + \frac{\partial \rho_B}{\partial t} - r_B = 0 \quad (12)$$

and $$\nabla . n_B + \frac{\partial \rho_B}{\partial t} - r_B = 0 \quad (13)$$

Adding equations (11) and (13), we obtained:

$$\nabla .(n_A + n_B) + \frac{\partial (\rho_A + \rho_B)}{\partial t} - (r_A + r_B) = 0 \quad (14)$$

But

$\eta_A + \eta_B = \rho_A V_A + \rho_B V_B = \rho V$ and $\rho_A + \rho_B = \rho$

Substituting these relations with equation (14)

$$\nabla . \rho V + \frac{\partial \rho}{\partial t} - (r_A + r_B) = 0 \quad (15)$$

Equation (15) represents the continuity equation for the mixture. Thus, writing equation (15) in substantial derivative gives:

$$\frac{D\rho}{Dt} + \rho \nabla . V = 0$$

$$\frac{\rho DW_A}{Dt} + \nabla . \rho_A - r_A = 0 \quad (16)$$

Molar equivalent of equations (11) and (13) are given as:

For component **A:**

$$\nabla N_A + \frac{\partial C_A}{\partial t} - R_A = 0 \quad (17)$$

For component B

$$\nabla N_B + \frac{\partial C_B}{\partial t} - R_B = 0 \quad (18)$$

Hence, for the mixture (addition of equation (17) and (18)) we have:

$$\nabla (N_A + N_B) + \frac{\partial (C_A + C_B)}{\partial t} - (R_A + R_B) = 0 \quad (19)$$

For a binary mixture

$N_A + N_B = C_A V_A + C_B V_B = CV$

and $C_A + C_B = C$

$A \rightleftharpoons B$, $R_A = -R_B$

$$\nabla . CV + \frac{\partial C}{\partial t} - (R_A + R_B) = 0 \quad (20)$$

Recall that:

$$N_A = -CD_{rB} \nabla . y_A + y_A (N_A + N_B)$$

$$= -CD_{AB} \left(\frac{\partial y_A}{\partial_x} + \frac{\partial y_A}{\partial_y} + \frac{\partial y_A}{\partial_z} \right) + y_A (N_A + N_B)$$

Or

$$N_A = -CD_{AB} \nabla y_A + C_A V \quad (21)$$

Substituting equation (15) into equation (11), we obtained

$$-\nabla . CD_{AB} \nabla y_A + \nabla . C_A V + \frac{\partial C_A}{dt} - R_A = 0 \quad (22)$$

http://ijses.com/
All rights reserved

$$-CD_{AB}\nabla^2 y_A + \nabla C_A V + \frac{\partial C_A}{\partial t} - R_A = 0$$

Equation (22) describes concentration problems within a diffusing system. This equation is relatively unwieldy. These equations can be simplified by making restrictive assumptions.

Assumptions:

If the density ρ and D_{AB} are constant

$$-CD_{AB}\nabla^2 y_A + V\nabla C_A + \frac{\partial C_A}{\partial t} - R_A = 0$$

$$-D_{AB}\nabla^2 C_A + V.\nabla C_A + \frac{\partial C_A}{\partial t} - R_A = 0$$

$$-D_{AB}\nabla^2 \rho_A + \rho_A \nabla.V + V.\nabla \rho_A + \frac{\partial \rho_A}{\partial t} - r_A = 0$$

Dividing each term by the molar weight of component **A** and rearranging we obtain

$$V.\nabla C_A + \frac{\partial C_A}{\partial t} = D_{AB}\nabla^2 C_A \pm R_A \tag{23}$$

$$V_x \frac{\partial C_A}{\partial x} + V_y \frac{\partial C_A}{\partial y} + V_z \frac{\partial C_A}{\partial z} + \frac{\partial C_A}{\partial t} = D_{AB}\left\{\frac{\partial^2 C_A}{\partial x^2} + \frac{\partial^2 C_A}{\partial y^2} + \frac{\partial^2 C_A}{\partial z^2}\right\} \pm R \tag{24}$$

The solution to equation (24) was solved numerically using the finite difference approximation (FDA) in the explicit scheme. Thus, resolving the resulting partial differential equation numerically and neglecting the flow of oxygen in y-direction, we obtain the following.

$$\frac{\partial C}{\partial t} = \frac{C_{i,j}^{k+1} - C_{i,j}^{k}}{\Delta t} \tag{25}$$

$$\frac{\partial C}{\partial z} = \frac{C_{i,j+1}^{k} - C_{i,j-1}^{k}}{2\Delta z} \tag{26}$$

$$\frac{\partial^2 C}{\partial x^2} = \frac{C_{i+1,j}^{k} - 2C_{i,j}^{k} + C_{i-1,j}^{k}}{\Delta x^2} \tag{27}$$

$$\frac{\partial^2 C}{\partial z^2} = \frac{C_{i,j+1}^{k} - 2C_{i,j}^{k} + C_{i,j-1}^{k}}{\Delta z^2} \tag{28}$$

The diffusion of oxygen in y-direction is minimal because of the driving force in the z direction, so the diffusion of oxygen in the y direction is insignificant. Hence, substituting equation (25) through equation (28) into (24) yields:

$$\frac{C_{i,j}^{k+1} - C_{i,j}^{k}}{\Delta t} = D\left[\frac{C_{i+1,j}^{k} - 2C_{i,j}^{k} + C_{i-1,j}^{k}}{\Delta x^2} + \frac{C_{i,j+1}^{k} - 2C_{i}^{k} + C_{i,j-1}^{k}}{\Delta z^2}\right] - v\left[\frac{C_{i,j+1}^{k} - C_{i,j-1}^{k}}{2\Delta z}\right] - R_{i,j}^{k} \tag{29}$$

For uniform grids $\Delta x = \Delta z$, therefore, equation (29) becomes:

$$C_{i,j}^{k+1} - C_{i,j}^{k} = \frac{\Delta tD}{\Delta x^2}\left(C_{i+1,j}^{k} - 2C_{i,j}^{k} + C_{i-1,j}^{k} + C_{i,j+1}^{k} - 2C_{i}^{k} + C_{i,j-1}^{k}\right) - \frac{\Delta tv}{2\Delta x}\left(C_{i,j+1}^{k} - C_{i,j-1}^{k}\right) - \Delta tR_{i,j}^{k} \tag{30}$$

Collection of like terms

$$C_{i,j}^{k+1} = \frac{\Delta tD}{\Delta x^2}\left(C_{i-1,j}^{k} + C_{i+1,j}^{k}\right) + \left(1 - 4\frac{\Delta tD}{\Delta x^2}\right)C_{i,j}^{k} + \left(\frac{\Delta tD}{\Delta x^2} + \frac{\Delta tv}{2\Delta x}\right)C_{i,j-1}^{k} + \left(\frac{\Delta tD}{\Delta x^2} - \frac{\Delta tv}{2\Delta x}\right)C_{i,j+1}^{k} - \Delta tR_{i,j}^{k} \tag{31}$$

Also, the reaction term $R_{i,j}^{k} = \frac{1}{Y}\frac{U_m SX}{K_s + S}$ and $S = C$.

Hence, $$R_{i,j}^{k} = \frac{1}{Y}\frac{U_m XC_{i,j}^{k}}{K_s + C_{i,j}^{k}} \tag{32}$$

Substituting equation (32) into (30) gives

http://ijses.com/
All rights reserved

International Journal of Scientific Engineering and Science
Volume 5, Issue 2, pp. 62-72, 2021. ISSN (Online): 2456-7361

$$C_{i,j}^{k+1} = \frac{\Delta tD}{\Delta x^2}\left(C_{i-1,j}^{k} + C_{i+1,j}^{k}\right) + \left(1 - 4\frac{\Delta tD}{\Delta x^2}\right)C_{i,j}^{k} + \left(\frac{\Delta tD}{\Delta x^2} + \frac{\Delta tv}{2\Delta z}\right)C_{i,j-1}^{k} + \left(\frac{\Delta tD}{\Delta x^2} - \frac{\Delta tv}{2\Delta z}\right)C_{i,j+1}^{k} + \Delta t\frac{1}{Y}\frac{U_m X C_{i,j}^{k}}{K_s + C_{i,j}^{k}} \quad (33)$$

Equation (33) is a numerical solution in two dimensional flows (x and z) to the model in the explicit scheme and it is the model for predicting the concentration of carbon dioxide produced with time and depth along the reactor.
Where C- initial oxygen concentration, D-diffusion coefficient of oxygen in the soil, Y- yield conversion constant, U_m - maximum specific growth rate, K_S – substrate saturation constant, Z- distance, t – time.
The initial and boundary conditions
At t = 0, $z \geq 0$ *and* $x \geq 0$: $C = 0$
At t > 0, $z = 0$ *and* $x = 0$: $C = C_0$
At t > 0, $z > 0$ *and* $x > 0$: $C = \infty$

III. Calculation Algorithm

The algorithm for implementation of the model solution is shown in Figure 1b as follows.

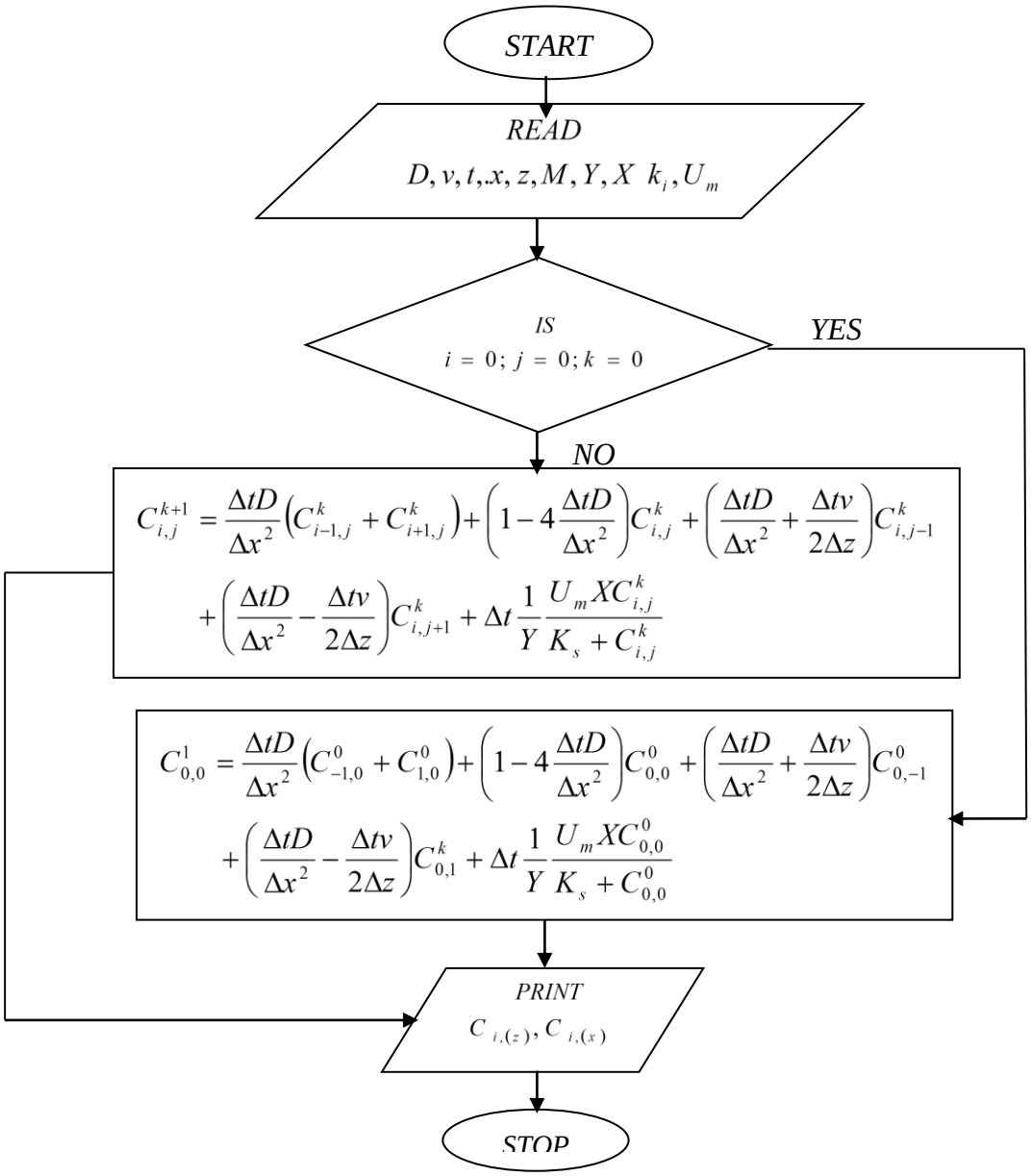

Figure 1b: Flow Algorithm for Predicting the Concentration of Carbon Dioxide Produced

http://ijses.com/
All rights reserved

IV. Results and Discussion

The simulated model results of concentration of carbon dioxide produced through the soil matrix is shown in surface plots. The experimental analyses of oxygen diffusion coefficient and velocities showed variation in the different soils (Umeda *et al*., 2018). Thus, the rate of carbon dioxide production in the soil types differs. Therefore, for sandy soil, the predicted concentration of carbon dioxide is shown in Figures 2 to 4. Similarly, the predicted concentration of carbon dioxide produced through sandy loam soil is shown in Figures 5 to 7, while Figures 8 to 10 shows the predicted concentration of carbon dioxide generating through clay soil over the investigative periods. In Figures 11 to 13, measured and predicted concentration of carbon dioxide produced were compared in the respective soils, while in Figure 14 comparison of carbon dioxide generated was made between the different soil media.

4.1. Surface Plot of Carbon Dioxide Produced in the Soils

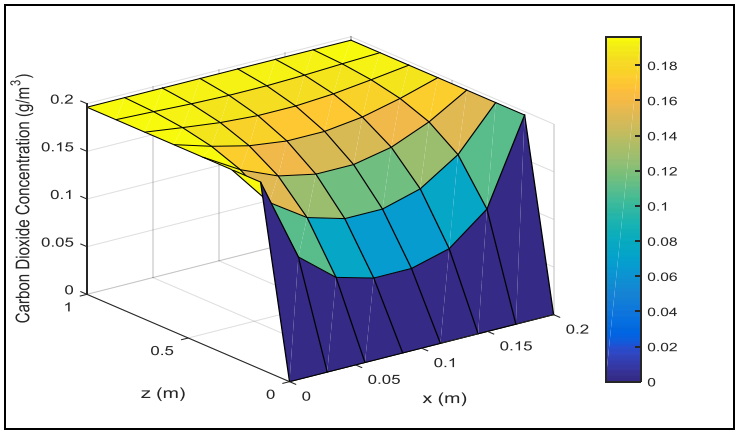

Figure 2: Concentration of Carbon Dioxide Produced in Sandy Soil (2 Weeks)

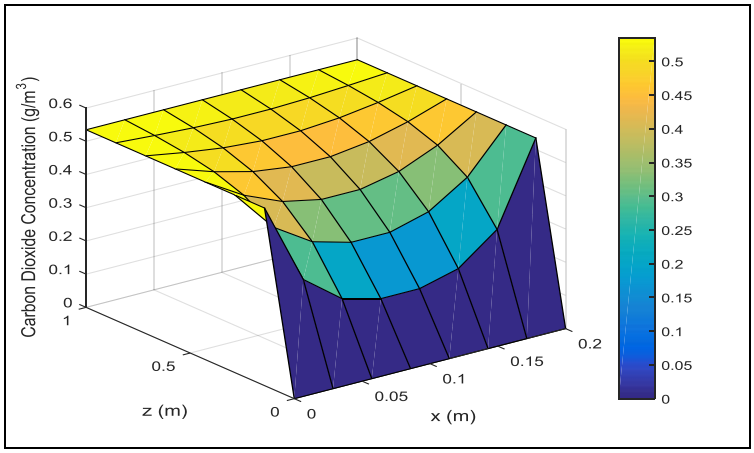

Figure 3: Concentration of Carbon Dioxide produced in Sandy Soil (4 Weeks)

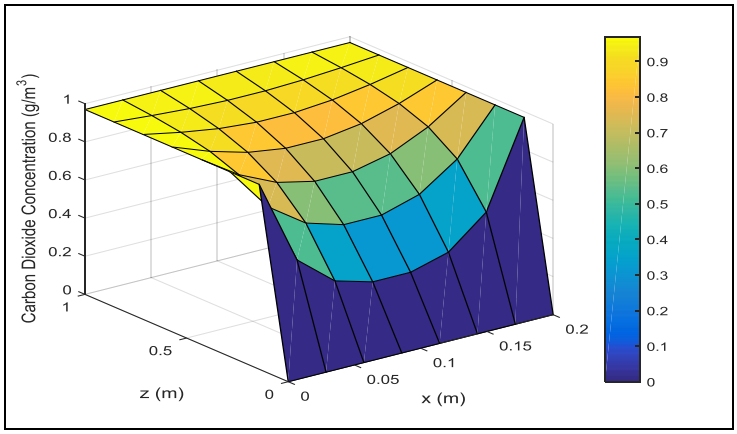

Figure 4: Concentration of Carbon Dioxide Produced in Sandy Soil (6 Weeks)

http://ijses.com/
All rights reserved

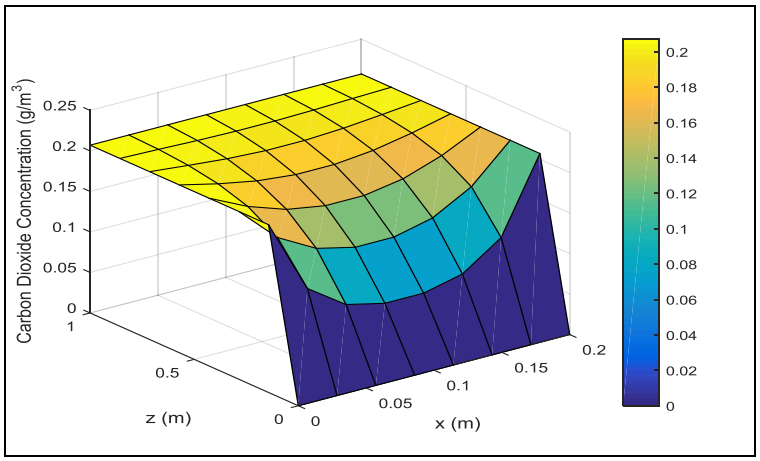

Figure 5: Concentration of Carbon Dioxide Produced in Sandy Loam Soil (2 Weeks)

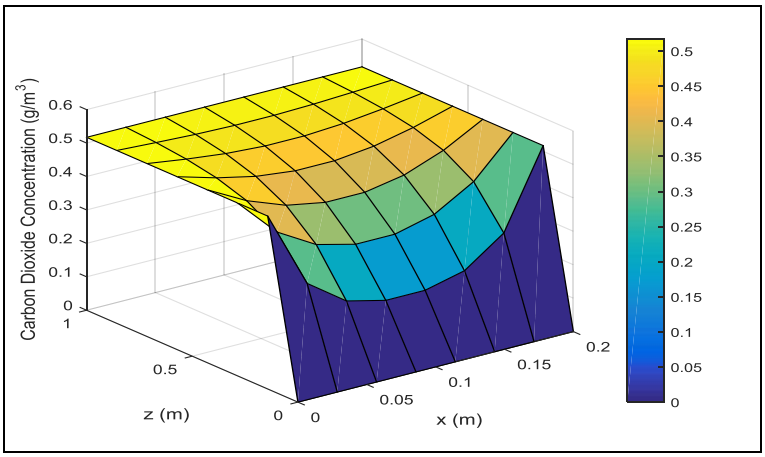

Figure 6: Concentration of Carbon Dioxide Produced in Sandy Loam Soil (4 Weeks)

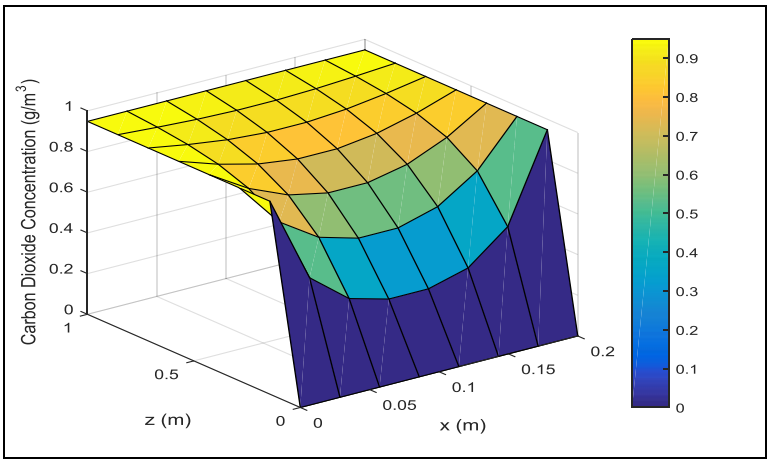

Figure 7: Concentration of Carbon Dioxide Produced in Sandy Loam Soil (6 Weeks)

http://ijses.com/
All rights reserved

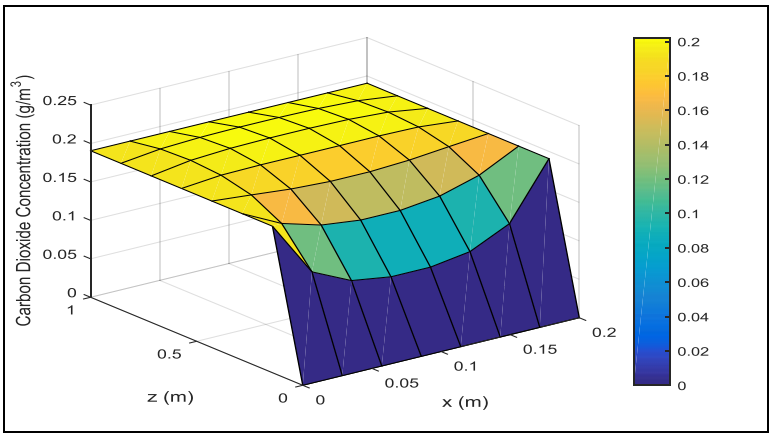

Figure 8: Concentration of Carbon Dioxide Produced in Clay Soil (2 Weeks)

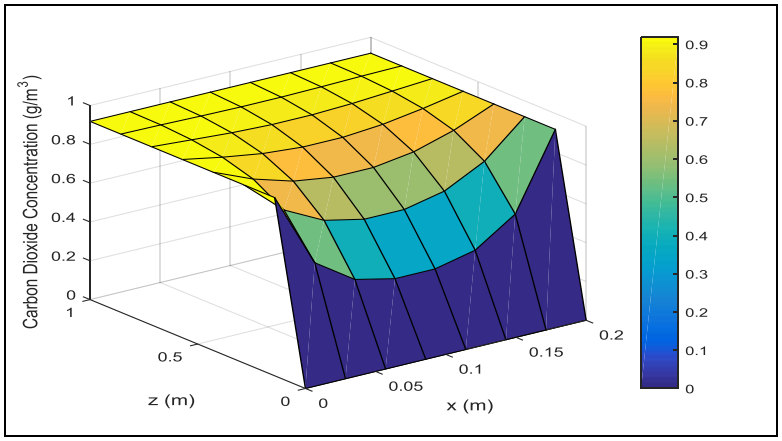

Figure 9: Concentration of Carbon Dioxide Produced in Clay Soil (4 Weeks)

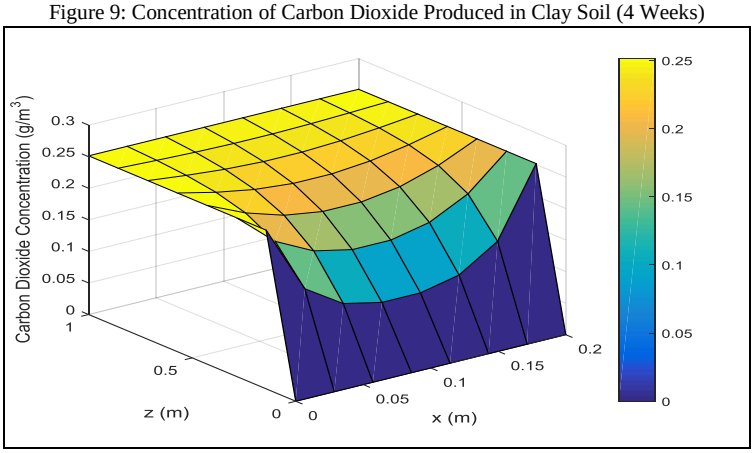

Figure 10: Concentration of Carbon Dioxide Produced in Clay Soil (6 Weeks)

Figure 2 through Figure 10 showed the surface plots of carbon dioxide concentration produced in x and z direction in Sandy, Sandy loam and Clay soils. The different colour as indicated in the graph showed the variations in concentration of the carbon dioxide as it evolved in x and z direction. The graph also indicated that the concentration of carbon dioxide produced increased with depth and time in x and z direction. The model results followed the same trends as obtained from the experiment, which implied that the developed model predicted the experimental results reasonably well.

4.2. Comparison between Experimental and Model Predictive Data for Carbon dioxide Concentration

The basis for comparison of the experimental and model data was to show the fitness of the data at all data point and the trend obtained from the experimental and predictive model results.

http://ijses.com/
All rights reserved

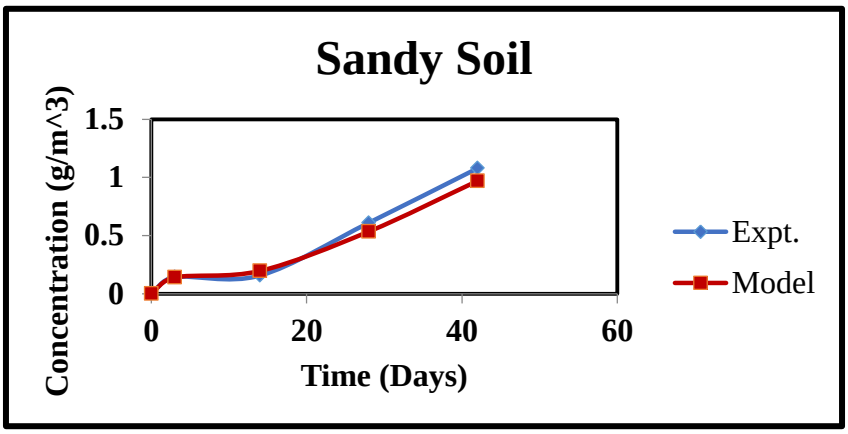

Figure 11:Comparison between Experimental and Model Predictive Data for Sandy Soils

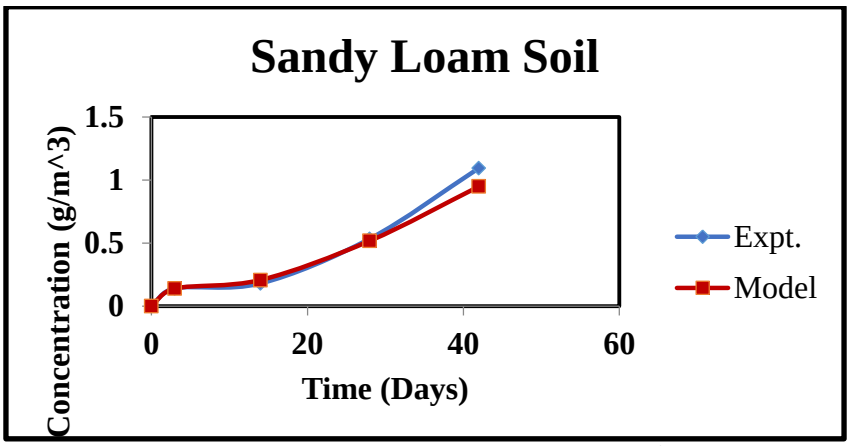

Figure 12: Comparison between Experimental and Model Predictive Data for Sandy Loam Soil

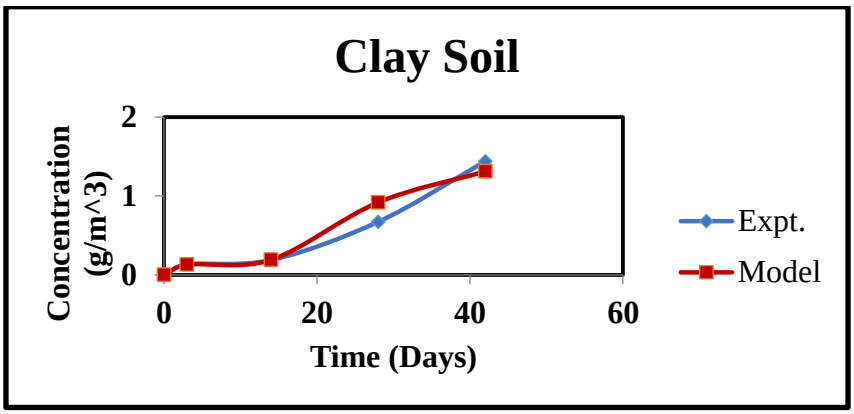

Figure 13: Comparison between Experimental and Model Predictive Data for Clay Soil

Figure 11 through Figure 13 indicated that the model gives very good fit of experimental data at all data points with an error of 0.09%, 0.08% and 0.05% for Sandy Soils, Sandy Loam Soil and Clay Soil respectively. Also, it showed that the results of the experimental and model followed the same trend. It was also noted that the rate of carbon dioxide production during the early stages after injection of oxygen into the reactor was slow, but increased rapidly as time progresses, and this was equally interpreted by the model as shown in the Figures.

4.3. Comparison of Carbon Dioxide Produced in Sandy Soils, Sandy Loam and Clay Soils

http://ijses.com/
All rights reserved

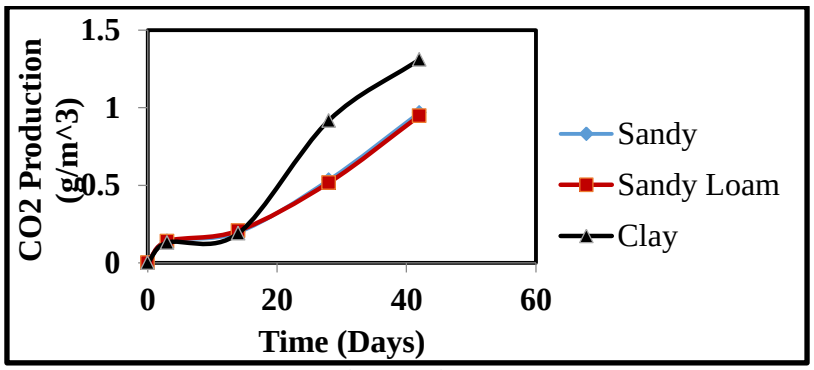

Figure 14: Comparison of Results of Carbon Dioxide Production

Figure 14 shows the graph of Carbon dioxide produced in sandy, sandy loam and clay soils. The results revealed that the production of carbon dioxide is highly appreciable in clay soil compared to sandy and sandy loam soils. This may be as a result of the particle size, surface area, and porosity of the soils.

4.4. Comparison of Results of Oxygen Diffusion and Carbon dioxide Produced in the Soils

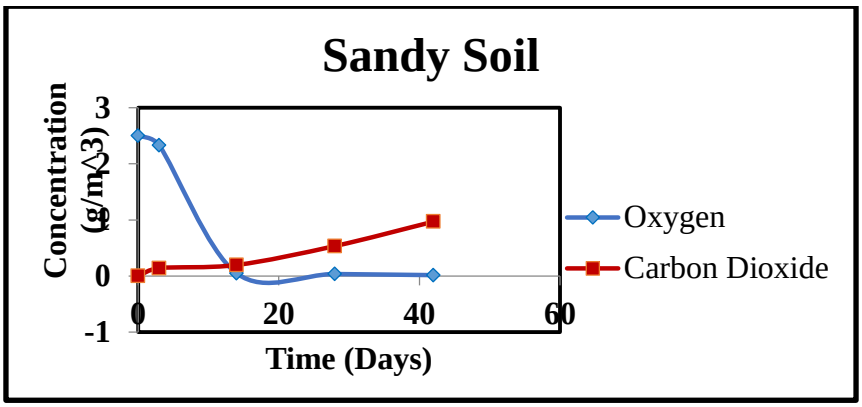

Figure 15:Comparison of Results of Oxygen Diffusion and Carbon Dioxide Produced in Sandy Soils

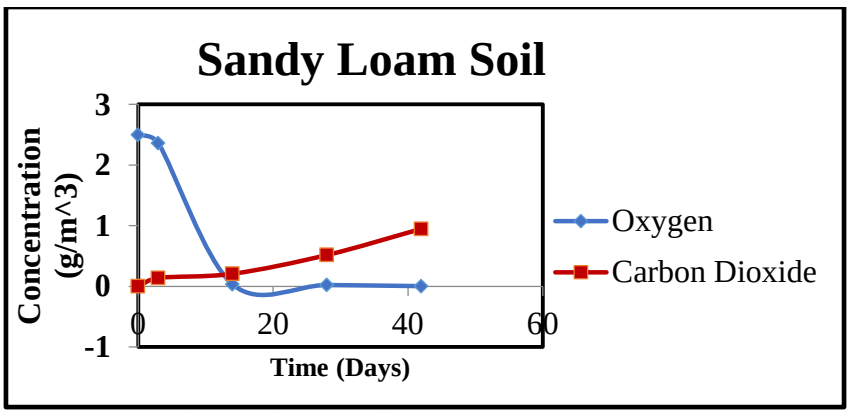

Figure 16. Comparison of Results of Oxygen Diffusion and Carbon Dioxide Produced in Sandy Loam Soils

All rights reserved

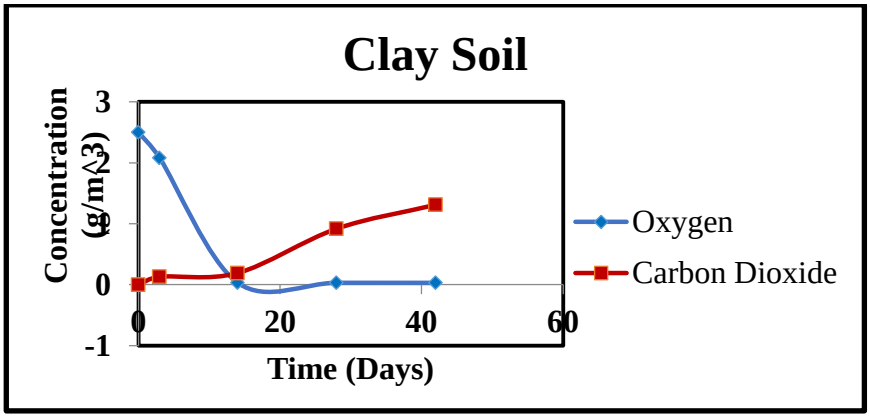

Figure 17: Comparison of Results of Oxygen Diffusion and Carbon Dioxide Produced in Clay Soils

Figures 15 – 17 show the graphs of Oxygen diffusion and Carbon dioxide produced in Sandy, Sandy loam and Clay soils respectively. The graphs revealed that, the Oxygen concentration in the soils deceased with time as it diffused through the soils while the concentration of carbon dioxide produced in the soils increased with time as the bioremediation process progressed. This implied that, the bioremediation process was effective and successful because the carbon dioxide produced is a byproduct of a successful bioremediation process (Ayotamuno, *et al.*, 2006).

V. CONCLUSION

Considering the results shown in this study, it become necessary to conclude that the developed mathematical model can be used for the prediction of carbon dioxide concentration generated or produced in two dimensional flows, for bioremediation of petroleum contaminated soils at 100cm depth at any given time.

REFERENCES

[1]. Abdulsalam, S. (2012). Mathematical Modeling of bioremediation of soil contaminated with spent oil. *Journal of Engineering Trends in Engineering and Applied Science*, 3, 654-659.
[2]. Aldrett, I., Bonner, S., Mills, J.S., Antenneth, M.A. & Stephen, R.L. (1997). Microbial degradation of crude oil in Marine environments tested in ask experiment. *Water Research*, 31, 2840-2848.
[3]. Chikere, C.B., Okpokwasili G.C., & Ichiakkor, O. (2009a). Characterisation of hydrocarbon utilizing bacteria in tropical marine sediments. *African Journal of Biotechnology*, 11, 2541-2544
[4]. Del Arco, J.P. & De Franca, F.P. (2001). Influence of oil contamination level on hydrocarbon biodegradation in sandy sediment. *Environmental Pollution*, 110, 515-519
[5]. Ezra, S., Feinstein, S., Pelly, I., Banman, D. & Miloslavsky, I. (2000). Weathering of fuel oil spill on the east Mediterranean coast, Ashdod, Isreal.*Organic Geochemistry*.3, 1733-1741.
[6]. Jose, N., Mauriscio, O., Luis M. & Edmound, A.(2015). Oxygen diffusion in soil: Understanding the factors and processes needed for modelling. *Chillean Journal of Agricultural Research*, 75, 35-44
[7]. Moldrup, P., Chamindu, T.K.K.D., Hamamoto, S., Komatsu, K. & Kawamato, D. E. (2013). Structure dependent water - induced linear reduction model for predicting gas diffusivity and tortuosity in repacked and intact soil. *Vadose Zone Journal*, 12, 1-11
[8]. Obando, F. (2003). Oxygen transport in waterlogged soils. Part II. Diffusion coefficients. College on Soil Physics, Trieste.3-21 March. International Centre for Theoretical Physics, Trieste, Italy.
[9]. Rahman, K.S.M., Thahira-Rahman, J., Lakshamapernmalsamy, P.& Banat, I. M. (2002). Towards efficient crude oil degradation by a mixed bacterial consortium. *Bio-resources Technology*, 85, 257 – 261.
[10]. Swannel, R.P.J.,Lee, K. & Mc Donagh, M. (1996). Field evaluation of marine oil spill bioremediation. *Microbiological Review*, 60, 343-365.
[11]. Umeda, U., Puyate, Y.T., Dagde, K.K. & Ehirim, E.O. (2017). Effect of oxygen diffusion on Total Petroleum Hydrocarbon in Petroleum contaminated soils. *International Journal of Engineering and Modern Technology*, 3(7), 18-24.
[12]. Umeda U., Puyate Y.T., Dagde K.K. & Ehirim, E.O. (2018). Development of predictive model for diffusion of oxygen through petroleum contaminated soils at 100cm depth. *International Journal of Engineering and Modern Technology*, 4(2), 42-53.
[13]. Van Hamme, J.D., Singh, A. & Ward, O.P. (2003). Recent advances in petroleum microbiology. *Microbial Molecular Biology Review*, 67, 503-549.
[14]. Valadi, M. (2001). Bioremediation: An overview. *Appl. Chem.*, 73, 1163 -1172.

http://ijses.com/
All rights reserved